REVIEW ARTICLES

Syntheses, crystal structure and magnetic properties of $R_{m+n}Co_{5m+3n}B_{2n}$ *

LIANG Jingkui (梁敬魁)[1,2,**], CHEN Yi (陈 怡)[1] and CHEN Xiaolong (陈小龙)[1]

1. Institute of Physics and Center for Condensed Matter Physics, Chinese Academy of Sciences, Beijing 100080, China

2. International Center for Materials Physics, Chinese Academy of Sciences, Shenyang 110015, China

Received May 15, 2001; revised June 19, 2001

Abstract The phase relations at the 600℃ and 700℃ isothermal sections of the ternary systems R-Co-B for R = Nd, Pr and R = Sm, Gd respectively were summarized in this paper. For $R_{m+n}Co_{5m+3n}B_{2n}$, two new types of compounds $R_3Co_{13}B_2$ (R = Pr, Nd, Sm, Gd, Dy, Ho, Er, Y) ($m = 2$, $n = 1$) and $R_5Co_{19}B_6$ (R = Pr, Nd) ($m = 2$, $n = 3$) were synthesized by utilizing the principle of structural combination. Their crystal structures and easy magnetization direction were determined by X-ray powder diffraction, and structures were refined by the Rietveld method. The Curie temperature T_C, saturation magnetization M_s and anisotropic field H_A of the new compounds were measured using a vibrating-sample magnetometer, an extraction sample magnetometer and $M(H) - H$ curves of samples in different magnetization directions respectively. The T_C and M_s of $R_{m+n}Co_{5m+3n}B_{2n}$ increase with increasing values of m at a given n value. H_A increases with an increase in n when m is kept invariable. The effects of the substitution of Ni for Co on the magnetic properties of $Nd_{13}Co_{15-x}Ni_xB_2$ were also investigated. It was found that T_{SR} decreased monotonously as the concentration of Ni increased, and at $x = 3$ the easy magnetization direction becomes axial at room temperature. The relations between crystal structure and magnetic properties of $R_{m+n}Co_{5m+3n}B_{2n}$ and the possible routes of synthesizing permanent magnetic materials are also discussed.

Keywords: **R-Co-B ternary systems, $R_3Co_{13}B_2$, $R_5Co_{19}B_6$, crystal structure, magnetic properties.**

R-Co-B ternary systems (R = rare earths, T = transition metals Fe, Co, Ni), especially the intermetallic compounds derived from RT_5 ($CaCu_5$ type structure) have attracted extensive attention in the exploration of new permanent magnetic materials since $Nd_2Fe_{14}B$ was discovered[1,2]. A series of $Sm_{1+n}Co_{5+3n}B_{2n}$ compounds with high anisotropic field H_A, such as $SmCo_5$ ($n = 0$), $SmCo_4B$ ($n = 1$), $Sm_3Co_{11}B_4$ ($n = 2$) and $SmCo_3B_2$ ($n = \infty$), have been found in the Sm-Co-B ternary system. H_A values of these compounds at 4.2 K are 71, 120, 116 and 130 T[3] respectively. However, the T_C and the M_s of these compounds are relatively low in these compounds. Partial substitution of Fe for Co, Pr for Sm and the introduction of interstitial N and C can further increase their M_s and T_C. But they are still too low to be used as permanent magnetic materials[4].

The subsolidus phase relations of R-Co-B (R = Ce, Pr, Nd, Sm, Gd, Dy, Er, Lu and Y) after long-time annealing at 400 ~ 800℃ have been reported by Kuzma et al.[5]. In these ternary systems, only $R_{1+n}T_{5+3n}B_{2n}$ with $n = 1$, 2, 3, and ∞ compounds were observed in their work. This series of

* Supported by Key Project of the National Natural Science Foundation of China (Grant No. 59631070) and the State Key Fundamental Research Projects by the Ministry of Science and Technology (Grant No. G1998061307-Re0204).

** Email: jkliang@aphy.iphy.ac.cn

compounds can be regarded as the stacking of one layer of RT_5 and n layers of RT_3B_2 (they all belong to hexagonal system, space group P6/mmm, $Z = 1$, 1a is occupied by 1R; 2c are occupied by 2T and 2B respectively; 3g equivalent points are all occupied by 3T) along the c-axis sharing a common plane through 3g equivalent points. Considering that RCo_5 is of ferromagnetism and RCo_3B_2 of diamagnetism, the H_A of these compounds can be enhanced by the substitution of B for Co in RCo_5. On the other hand, the T_C and the M_s decrease rapidly due to the hybridization of 2p electrons of B and 3d of Co. We tried to improve the synthesizing method to increase the relative concentrations of Co and Fe in the compounds while keeping the H_A high. New compounds alternative stacking of m layers of RT_5 and n layers of RT_3B_2 along the c-axis are expected to synthesize. This work is supported through a key project "research of new type of rare earth function material" by the National Natural Science Foundation of China (NNSFC). A comprehensive report about the phase relations of R-Co-B ternary systems, crystal structures and magnetic properties of $R_{m+n}Co_{5m+3n}B_{2n}$ compounds and $R_3Co_{13-x}Ni_xB_2$ system is presented here.

1 Phase relations of R-Co-B ternary systems (R = Pr, Nd, Sm, Gd)

The starting materials are rare earth R, Co and CoB alloys with a purity better than 99.9%. In the Co-rich part (the concentration of Co is higher than those of $NdCo_2$ and CoB) of the ternary system R-Co-B (R = Pr, Nd, Sm, Gd), approximately fifty samples were prepared from an appropriate amount of the starting metallic materials in each system[6~9]. To ensure the homogeneity of the samples, the ingot was turned and melted 5 ~ 6 times in an electric arc furnace. The weight loss of the samples was less than 1% (the loss of Sm may reach up to 50% by chemical analysis). These samples are annealed in vacuum at 600℃ (R = Pr, Nd) or 700℃ (R = Sm, Gd) for 3 or 4 months and then cooled down to room temperature rapidly. The isothermal section diagrams of R-Co-B (R = Pr, Nd, 600℃) and R-Co-B (R = Sm, Gd 700℃) are established by X-ray phase identification.

1.1 R-Co-B (R = Pr, Nd) ternary system

There exist binary compounds and 11 ternary compounds with an identical structure type in the Co-rich part of Nd-Co-B and Pr-Co-B ternary systems. The phase relations in the isothermal sections of the two systems are the same. The lattice parameters of the same compounds keep constant in different 3-phase areas and no detectable solid solution region exists in the diagram, indicating that the ternary compounds are stoichiometric compounds with identical chemical compositions. So the two-phase regions degenerate to lines. In Fig. 1(a) the triangle areas correspond to the three-phase regions and the lines linking two phases are the two-phase equilibrium regions.

Our isothermal section of R-Co-B (R = Pr, Nd) ternary system is quite different from that of Ref. [5]. Only nine kinds of ternary compounds have been observed in the composition range we have studied. R_2Co_9B (R = Pr, Nd) has not been found in our work. No crystal structure and X-ray diffraction data of this ternary compound are given in Ref. [5]. According to our phase diagram, the composition (R_2Co_9B) is in the two-phase region which consists of RCo_5 and $R_3Co_{13}B_2$. Moreover, we have successfully synthesized 3 ternary compounds which have not been reported in Ref. [5] in R-Co-B ternary system, i.e. $R_3Co_{13}B_2$, $R_5Co_{19}B_6$ and $R_2Co_{14}B$. So there exist differences between the results of Ref. [5] and ours in the division of three-phase regions and links of two-phase regions.

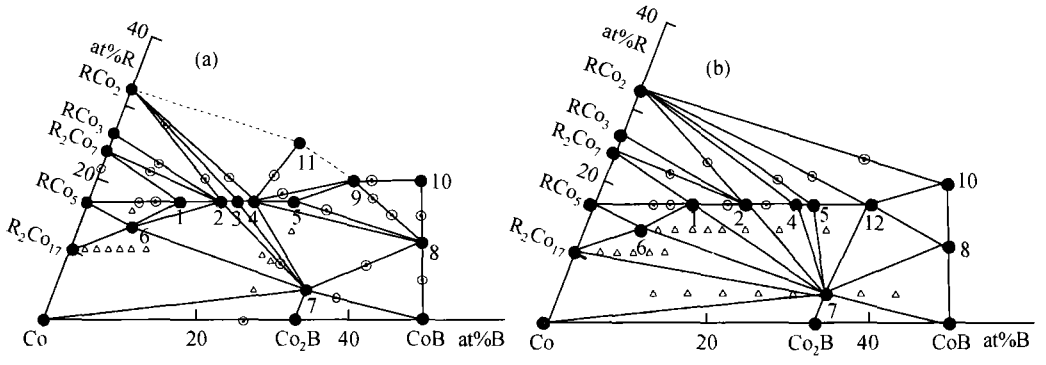

Fig. 1 The phase relations in the isothermal sections of R-Co-B ternary systems. (a) R = Pr, Nd at 600℃; (b) R = Sm, Gd at 700℃. ●, single phase; ⊙, two phases; △, three phases. 1, $R_3Co_{13}B_2$; 2, RCo_4B; 3, $R_5Co_{19}B_6$; 4, $R_3Co_{11}B_4$; 5, $R_2Co_7B_3$; 6, $R_2Co_{14}B$; 7, $RCo_{12}B_6$; 8, RCo_4B_4; 9, $R_2Co_5B_3$; 10, RCo_2B_2; 11, $R_2Co_5B_2$; 12, RCo_3B_2.

1.2 R-Co-B (R = Sm, Gd) ternary system

The phase relations in isothermal sections at 700℃ at the Co-rich part of the Sm-Co-B and Gd-Co-B systems are identical with each other and they are a little different from those of R-Co-B (R = Pr, Nd) system. In the studied composition range, only nine ternary compounds have been observed, but RCo_3B_2 (R = Sm, Gd) have been not observed in the R-Co-B (R = Pr, Nd) systems. $R_5Co_{19}B_6$, $R_2Co_5B_3$ and $R_2Co_5B_2$ which have been observed in the R-Co-B (R = Pr, Nd) systems are also not detected in Sm (Gd)-Co-B systems. As in Pr (Nd)-Co-B systems, the compounds that lie in different 3-phase regions have constant lattice parameters. This result shows that there are no observable solid solution regions in the phase diagrams of these compounds, which are stoichiometric compounds with identical compositions.

Compared with the results of Ref. [5], seven ternary compounds were observed in the composition range of our study, i.e. RCo_4B, $R_3Co_{11}B_4$, $R_2Co_7B_3$, RCo_3B_2, $RCo_{12}B_6$, RCo_4B_4 and RCo_2B_2. Two compounds, $R_3Co_{13}B_2$ and $R_2Co_{14}B$, have been observed in our work, which had not been reported in Ref. [5]. Three ternary compounds reported in Ref. [5], R_2Co_9B, $R_5Co_8B_5$ and $R_2Co_5B_2$, have not been found in this study. So there are differences in the division of the phase diagram between the results of Ref. [5] and ours.

Two new compound families, $R_3Co_{13}B_2$ (R = Pr, Nd, Sm, Gd, Dy, Ho, Er, and Y) and $R_5Co_{19}B_6$ (R = Pr, Nd) have been successfully synthesized in the $R_{m+n}Co_{5m+3n}B_{2n}$ system under the conditions of relatively low temperatures (600 ~ 700℃) and long-time annealing (4 ~ 6 months), which have never been reported. They are probable products of the peritectic reactions of $RCo_5 + 2RCo_4B = R_3Co_{13}B_2$ and $2RCo_4B + R_3Co_{11}B_4 = R_5Co_{19}B_6$ at temperatures lower than 800℃. The reaction temperature cannot be measured accurately with thermal analysis method because of the sluggish reaction speed. In general, light rare earth elements are apter to form compounds with $m \geqslant 2$ than heavy ones. The bigger the value of m, the more difficult the synthesis. In addition to long time annealing at low temperatures, some processes are also effective to fabricating compounds with $m \geqslant 2$ such as mechanical alloying and non-crystallizing, melting non-crystallizing and heat treating at

appropriate temperatures. The phase diagrams of R-Co-B need further study.

2 Crystal structure and magnetic properties of $R_{m+n}Co_{5m+3n}B_{2n}$ compounds

2.1 Crystal structures of $R_{m+n}Co_{5m+3n}B_{2n}$ compounds

$R_{m+n}Co_{5m+3n}B_{2n}$, which derives from the structure of RCo_5, is formed by alternate stacking of m layers of RCo_5 and n layers of RCo_3B_2 along the Z-axis combined by the plane of 3g equivalent points in P6/mmm space group occupied by 3 Co atoms. The crystal structures of $R_{m+n}Co_{5m+3n}B_{2n}$ compounds are shown in Fig. 2, of which two new types ($m = 2$, $n = 1$ and $m = 2$, $n = 3$) in P6/mmm space group are first synthesized in this study[10~13]. The lattice parameters are shown in Table 1. Basically, $a \approx a_0$, although a slightly increases with increasing m and n, and c increases with m and n via $c \approx mc_0 + nc'$. a_0 and c_0 are the lattice parameters of RCo_5, $a_0 \approx 5.1$Å $c_0 \approx 3.955$Å, and c' is the parameter of RCo_3B_2 ($c' \approx 2.930$Å).

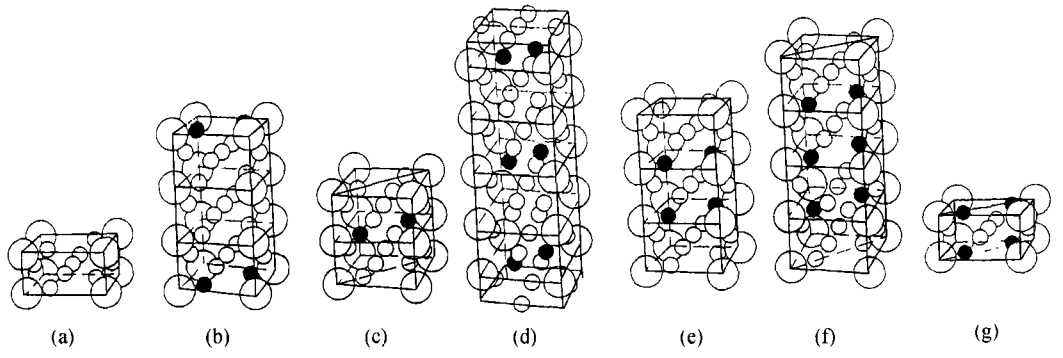

Fig. 2 Crystal structure of synthesized compounds $Nd_{m+n}Co_{5m+3n}B_{2n}$. ○ rare earth, ○ Co, ● B atom. (a) RCo_5 ($m = 1$, $n = 0$), (b) $R_3Co_{13}B_2$ ($m = 2$, $n = 1$), (c) RCo_4B ($m = 1$, $n = 1$), (d) $R_5Co_{19}B_6$ ($m = 2$, $n = 3$), (e) $R_3Co_{11}B_4$ ($m = 1$, $n = 2$), (f) $R_2Co_7B_3$ ($m = 1$, $n = 3$), (g) RCo_3B_2 ($m = 0$, $n = 1$).

Table 1 Ternary compounds in R-Co-B systems (R = Pr, Nd, Sm, and Gd)[a]

No.	Compound	Structure type	Space group	Observed rare earth borides	Lattice parameters		
					a(Å)	b(Å)	c(Å)
1	$R_3Co_{13}B_2$	$La_3Ni_{13}B_2$	P6/mmm	R = Pr, Nd, Sm, Gd	5.089		10.818
2	RCo_4B	$CeCo_4B$	P6/mmm	R = Pr, Nd, Sm, Gd	5.086		6.901
3	$R_5Co_{19}B_6$	New type	P6/mmm	R = Pr, Nd	5.133		16.652
4	$R_3Co_{11}B_4$	$Ce_3Co_{11}B_4$	P6/mmm	R = Pr, Nd, Sm, Gd	5.140		9.742
5	$R_2Co_7B_3$	$Ce_2Co_7B_3$	P6/mmm	R = Pr, Nd, Sm, Gd	5.159		12.767
6	$R_2Co_{14}B$	$Nd_2Fe_{14}B$	$I4_2/mnm$	R = Pr, Nd, Sm, Gd	8.646		11.865
7	$RCo_{12}B_6$	$SrNi_{12}B_6$	R3m	R = Pr, Nd, Sm, Gd	9.502		7.471
8	RCo_4B_4	$NdCo_4B_4$	$P4_2/n$	R = Pr, Nd, Sm, Gd[b]	7.070		3.822
9	$R_2Co_5B_3$	New type	Cccc	R = Pr, Nd	5.130	38.2	10.770
10	RCo_2B_2	$BaAl_4$	I4/mmm	R = Pr, Nd, Sm, Gd	3.586		9.747
11	$R_2Co_5B_2$	$Ce_2Co_5B_2$	$P6_3/mmc$	R = Pr, Nd	5.115		20.565
12	RCo_3B_2	$Ce_2Co_3B_2$	P6/mmm	R = Sm, Gd	5.079		3.031[c]

a) In the table lattice parameters obtained for R = Nd decrease with decreasing R atom radius. Pr radius is close to that of Nd.

b) $GdCo_4B_4$ belongs to $CeCo_4B_4$ structure type with space group $P4_2/nmc$.

c) The lattice parameters are obtained from R = Gd.

$R_3Co_{13}B_2$(R = Pr, Nd, Sm, Gd, Dy, Ho, Er, Y) with $m = 2$, $n = 1$ and $R_5Co_{19}B_6$(R = Pr, Nd) with $m = 2$, $n = 3$ are two series of compounds with new structural types. They all belong to the space group P6/mmm. Each unit cell contains one formula. The crystal structures of $Nd_3Co_{13}B_2$ and $Nd_5Co_{19}B_6$ determined by X-ray diffraction and refined with Rietveld technique are shown in Tables 2 and 3. The residual factors R_p for $Nd_3Co_{13}B_2$ and $Nd_5Co_{19}B_6$ are 12.5% and 13.6% respectively. The atomic parameters of other isostructural rare-earth compounds are similar. Fig. 3 (a), (b) is the X-ray powder diffraction patterns of $Nd_3Co_{13}B_2$ and $Nd_5Co_{19}B_6$ with Cu Kα radiation.

Table 2 Crystal structure and atomic distance of nearest neighbors for $Nd_3Co_{13}B_2$ P6/mmm, $a = 5.0722$ (4), $c = 10.7840$ (5)Å

Atom	Site	Position			Nearest neighboring atoms	Average atomic distances(Å)				
		x/a	y/b	z/c		Nd-Nd	Nd-Co	Nd-B	Co-Co	Co-B
1Nd(1)	1a	0	0	0	2Nd(2) + 12Co(2) + 6B	3.550	2.922	2.928		
2Nd(2)	2e	0	0	0.329	1Nd(1) + 1Nd(2) + 6Co(1) + 12Co(2)	3.617	3.172			
4Co(1)	4h	1/3	2/3	0.3159	3Nd(2) + 3Co(1) + 3Co(3)		2.932		2.698	
6Co(2)	6i	1/2	0	0.1346	2Nd(1) + 2Nd(2) + 4Co(2) + 2Co(1) + 2B		3.107		2.505	2.061
3Co(3)	3g	1/2	0	1/2	4Nd(2) + 4Co(3) + 4Co(1)		3.134		2.502	
2B	2c	1/3	2/3	0	3Nd(1) + 6Co(2)			2.928		2.062

Table 3 Crystal structure and atomic distance of nearest neighbors for $Nd_5Co_{19}B_6$, P6/mmm, $a = 51328$ (3), $c = 16.6519$ (5)Å

Atom	Site	Position			Nearest neighbors	Average atomic distances(Å)				
		x/a	y/b	z/c		Nd-Nd	Nd-Co	Nd-B	Co-Co	Co-B
1Nd(1)	1b	0	0	1/2	2Nd(2) + 12Co(2) + 6B(1)	3.370	2.960	2.963		
2Nd(2)	$2e_1$	0	0	0.2976	1Nd(1) + 1Nd(3) + 6Co(1) + 6Co(2) + 6Co(3)	3.360	3.147			
2Nd(3)	$2e_2$	0	0	0.0964	1Nd(2) + 1Nd(3) + 6Co(3) + 6Co(4) + 6B(2)	3.281	2.951	2.694		
4Co(1)	$4h_1$	1/3	2/3	0.2955	3Nd(2) + 3Co(2) + 3Co(3)		2.964		2.469	
6Co(2)	$6i_1$	1/2	0	0.4114	2Nd(1) + 2Nd(2) + 4Co(2) + 2Co(1) + 2B(1)		3.075		2.522	2.091
6Co(3)	$6i_2$	1/2	0	0.1742	2Nd(2) + 2Nd(3) + 4Co(3) + 2Co(1) + 2B(2)		3.081		2.546	1.999
3Co(4)	3f	1/2	0	0	4Nd(3) + 4Co(4) + 4B(2)		3.027		2.566	2.151
2B(1)	2d	1/3	2/3	1/2	3Nd(1) + 6Co(2)			2.963		2.091
4B(2)	$4h_2$	1/3	2/3	0.0936	3Nd(3) + 3Co(3) + 3Co(4)			2.964		2.075

According to Tables 2 and 3, the Co (1) and Co (2) in $Nd_3Co_{13}B_2$ deviate about 0.188Å and 0.35Å from their ideal positions respectively while the Co (2) and Co (3) in $Nd_3Co_{13}B_2$ deviate about 0.190Å and 0.450Å respectively with remaining atoms basically in ideal positions. This will make the distances between Nd or B atoms, which are adjacent to Co in the c direction, longer or shorter than their normal values. Furthermore the abnormal inter-atomic distances will affect the stability and magnetic properties of compounds. The compounds of $R_{m+n}Co_{5m+3n}B_{2n}$ ($m \geqslant 2$) are hard to be synthesized because of their low stability. They can be fabricated only by long-time annealing below the peritectic temperature. The decomposition above peritectic temperature makes great difficulties in syntheses of these compounds. $R_5Co_{19}B_6$ is more difficult to be synthesized than $R_3Co_{13}B$ because of the larger deviations of its part atoms from their ideal positions.

2.2 Magnetic properties of $R_{m+n}Co_{5m+3n}B_{2n}$

The temperature dependence of the magnetization $M(T)$ of the $Nd_{m+n}Co_{5m+3n}B_{2n}$ powder

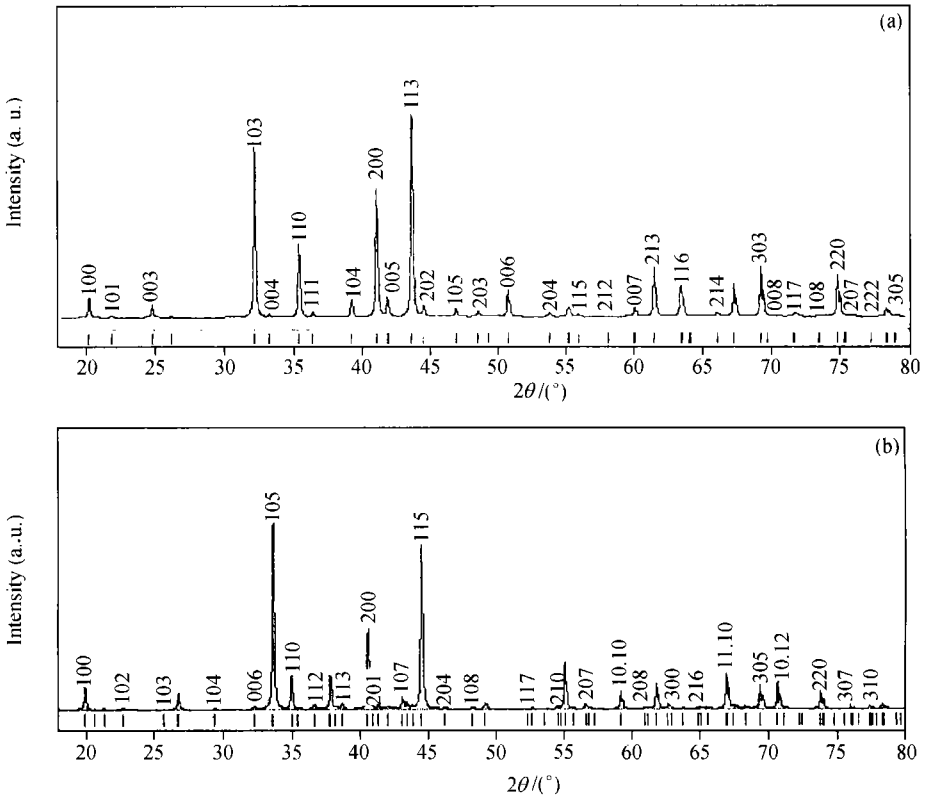

Fig. 3 XRD patterns for $Nd_3Co_{13}B_2$(a) and $Nd_5Co_{19}B_6$(b) with Cu Kα radiation. The vertical bars at the bottom indicate the position of the diffraction lines.

sample is illustrated in Fig. 4. The measurement was performed in a low field of 0.05 T with a vibrating sample magnetometer. The Curie temperatures T_C (Table 4) are determined from $M^2 - T$ plots by extrapolating M^2 to zero. Due to the increase in B concentration which weakens the Co-Co interaction and the enhancement of magnetic dilution of B, the Curie temperature decreases monotonically with increasing B concentration. When m keeps constant, T_C decreases with an increase in n. When n is invariable, T_C increases with increasing m. The spin-reorientation temperatures of $Nd_3Co_{13}B_2$($m = 2$, $n = 1$) and $Nd_3Co_{11}B_4$($m = 1$, $n = 2$) have been determined to be 370 and 110 K respectively.

The magnetization curves $M(H)$ of $Nd_{m+n}Co_{5m+3n}B_{2n}$(size of powder sample < 40 μm) were measured with an extraction sample magnetometer at 5 K in fields ranging from 0 to 5.17×10^6 A/m. The saturation moments M_s were deduced from $M - 1/H$ plot by extrapolating $1/H$ to zero. The results are shown in Table 4. The coupling of magnetic moments in $Nd_{m+n}Co_{5m+3n}B_{2n}$ compounds is similar to that of Nd-Co binary compounds. The magnetic moments of Nd is parallel to that of Co. Magnetic moments per chemical formula $Nd_{m+n}Co_{5m+3n}B_{2n}$ is $\mu_s = (m + n)\mu_{Nd} + (5m + 3n)\mu_{Co}$. Here μ_{Nd} and μ_{Co} are the average magnetic moments of Nd and Co, respectively. There are three different types of Co coordination to B atoms in $Nd_{m+n}Co_{5m+3n}B_{2n}$ structures. All these Co atoms have different average magnetic moments. Co(0), Co(1) and Co(2) represent the Co atoms whose

adjacent higher and lower layers have no B, one layer containing B and both layers containing B, respectively.

$Nd_3Co_{13}B_2$ ($m = 2$, $n = 1$),

$$\mu_{Co} = [4\mu_{Co(0)} + 3\mu_{Co(0)} + 6\mu_{Co(1)}]/13,$$

$Nd_5Co_{19}B_6$ ($m = 2$, $n = 3$),

$$\mu_{Co} = [4\mu_{Co(0)} + 6\mu_{Co(1)} + 6\mu_{Co(1)} + 3\mu_{Co(2)}]/19.$$

Other compounds ($m = 1$),

$$\mu_{Co} = [2\mu_{Co(0)} + 6\mu_{Co(1)} + 3(n-1)\mu_{Co(2)}]/(3n+5).$$

The atomic magnetic moment of Nd^{3+} is assumed reasonably to be $3\mu_B$[14]. Then we get $\mu_{Co(0)} = 1.2\ \mu_B$[15] in terms of the magnetic moments of $NdCo_5$. The filling of valence electrons of B atoms in Co (2)-3d orbits results in $\mu_{Co(2)} = 0$ as in compound $NdCo_3B_2$[16]. The calculated magnetic moments of Co in different positions are listed in Table 4. The average magnetic moments of Co (μ_{Co}) decreases with increasing B. This result is consistent with the decrease in the density of states at the Fermi energy due to the p-d orbital hybridization and the decreasing split based on the results of band structure calculations of the 3d band[17]. $\mu_{Co(1)}$ varies with B concentration and reaches a minimum at 20 at% B. Although μ_{Co} decreases with B concentration, the calculated $\mu_{Co(1)}$ increases because $\mu_{Co(2)}$ has been assumed to be zero.

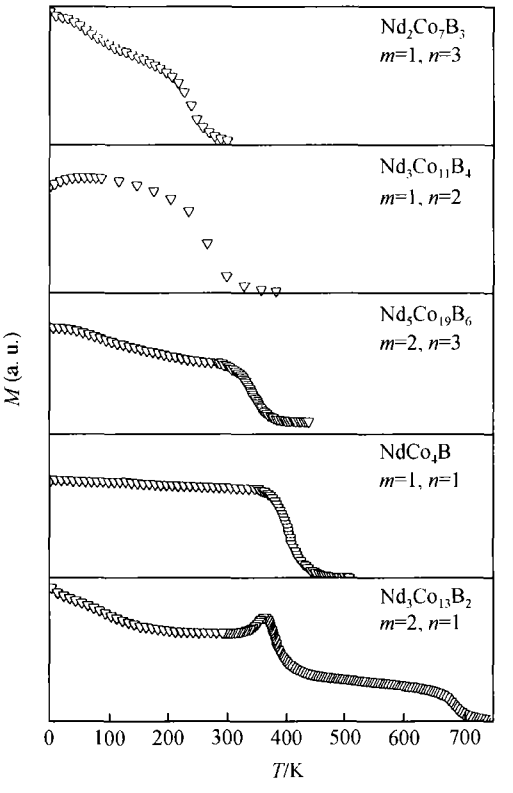

Fig. 4 Manetization-temperature curves of $Nd_{m+n}Co_{5m+3n}B_{2n}$ powder under a field of 0.05 T.

Table 4 Magnetic properties for $Nd_{m+n}Co_{5m+3n}B_{2n}$

Compound	T_C /K	T_{SR} /K	B /at%	M_S/(5K) (μ_B/fu)	μ_{Co} (μ_B/at)	$\mu_{Co(0)}$ (μ_B/at)	$\mu_{Co(1)}$ (μ_B/at)	$\mu_{Co(2)}$ (μ_B/at)	H_A(5K) /10^6 A·m^{-1}	EMD /298 K
$NdCo_5$	910	-	0	9.1	1.22	1.2	-	-	2.4	Plane
$Nd_3Co_{13}B_2$	710	370	11.1	20.8	0.91	1.2	0.57	-	14.3	Plane→axis
$NdCo_4B$	460	-	16.7	5.8	0.70	1.2	0.53	-	8.0	Axis
$Nd_5Co_{19}B_6$	380	-	20.0	21.5	0.34	1.2	0.14	0	27.1	Plane
$Nd_3Co_{11}B_4$	350	100	22.2	12.4	0.31	1.2	0.17	0	39.0	Cone→plane
$Nd_2Co_7B_3$	320	-	25.0	8.0	0.29	1.2	0.27	0		Plane

The method to measure the magnetocrystalline anisotropy is as follows: the mixture of the fine powder sample and epoxy resin in 1 : 1 weight proportion was pressed into thin pellets. Then the aligning was done by allowing the pellets to harden in a vertical magnetic field of 1T at room temperature for 6 h. Then these samples with solidified epoxy resin were analyzed by X-ray diffraction. The X-ray diffraction patterns are presented in Fig. 5 from which easy-magnetization direction (EMD) (Table 4) can be determined. The Spin-reorientation from easy-basal-plane to easy-

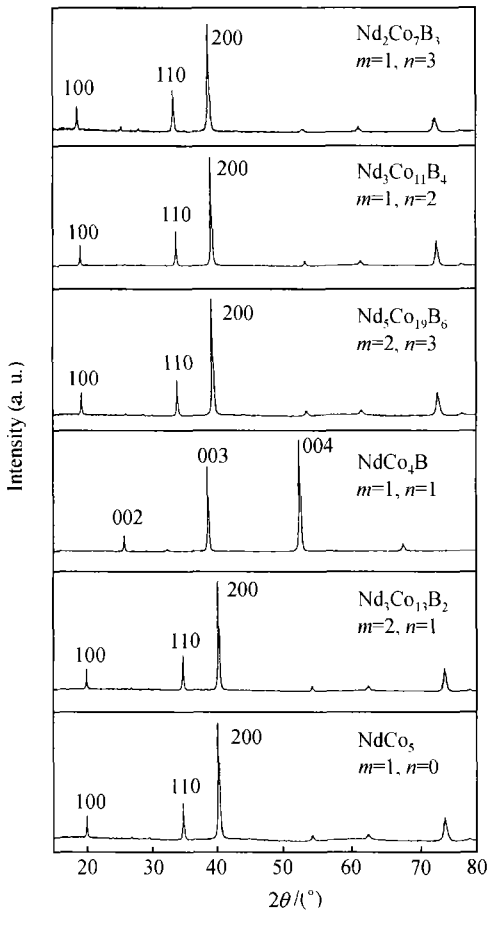

Fig. 5 XRD patterns of magnetically aligned $Nd_{m+n}Co_{5m+3n}B_{2n}$ at room temperature.

axis anisotropy for $Nd_3Co_{13}B_2$ was observed at 370 K. Spin-reorientation from easy-cone anisotropy to easy-basal-plane for $Nd_3Co_{11}B_4$ was observed at 100 K. The magnetic diagram of $Nd_{m+n}Co_{5m+3n}B_{2n}$ is plotted in Fig. 6. The spin-reorientations were also observed for compounds in $Pr_{m+n}Co_{5m+3n}B_{2n}$ family. However, the T_{SR} values are much lower. For $Pr_3Co_{13}B_2$, the T_{SR} is about 300 K, and its easy magnetization direction is the c axis at room temperature.

The methods of measuring the anisotropic field H_A are as follows: fine powder mixture of samples and epoxy resin in 1 : 1 weight ratio was put into a plastic tube with inner diameter of about 3.5 mm. The samples with easy-basal-plane anisotropy were aligned at a 1T field which is perpendicular to the axis direction of the plastic tube. The magnetic orientation lasted for 6 h while the sample tubes were kept rotating. For samples with easy-axis anisotropy, magnetic orientation was carried out with static method. In the procedure of magnetic orientation the axis of the sample tube was parallel to the magnetic field of 1 T for 6 h. Samples were taken out after the epoxy resin have been solidified. Then the $M_{//} - H$ and $M_{\perp} - H$ curves were measured. The extrapolated intersection point of linear parts of easy magnetization and hard magnetization curves was determined to be anisotropic field, H_A values. The results are listed in Table 4. H_A values increase with the concentration of B with the exception of $NdCo_4B$ in easy-axis direction.

3 Structure and magnetic properties of $Nd_3Co_{13-x}Ni_xB_2$

$Nd_3Co_{13}B_2$ has relatively high Curie temperature and saturation magnetization in the $Nd_{m+n}Co_{5m+3n}B_{2n}$ compounds. However, this compound exhibits an easy-basal-plane anisotropy which restricts its application as a permanent magnet. According to related reports, RT_5 of $CaCu_5$ type and its derivatives might change their magnetic anisotropy and other magnetic properties through partial substitution of other metal elements for transition metals. Elements such as Fe, Ni, Cu, Al and Si, have been used to substitute Co in $Nd_3Co_{13}B_2$. The structures and magnetic properties of these compounds have been studied. It is found that Ni can substitute Co in large amount and has a profound effect on the magnetic properties of this compound.

A series of $Nd_3Co_{13-x}Ni_xB_2$ ($x = 0, 1.0, 2.0, 3.0, 4.0, 5.0$) alloys were prepared with arc-melting method, and annealed at 600℃ for 2 months[18]. The samples were all determined to be pure-phase $Nd_3Co_{13}B_2$ solid solutions. The solid solubility of Ni in $Nd_3Co_{13-x}Ni_xB_2$ is about $x = 5$. The change of lattice parameters with Ni content is shown in Table 5. The influence of Ni content on lattice parameters is anisotropic: a decreases while c increases. The lattice parameter a decreases linearly as $a = a_0 - 0.031x$ ($x \leqslant 5$) while c increases linearly as $c = c_0 + 0.220x$ when $x \leqslant 3$ and then increases slowly. The cell volume v increases with x as $v = v_0 + 0.20x$ when $x < 4$ and then it remains essentially constant with x. The atom radii of Co and Ni are 1.25Å and 1.24Å respectively. The variation of lattice parameters may indicate the preferred substitution of Ni for Co. But it is hard to determine by X-ray diffraction due to the close values of scatter factor for Co and Ni. In addition, because of the large neutron absorption coefficients of Co and B, its structure can hardly be determined by the neutron diffraction method.

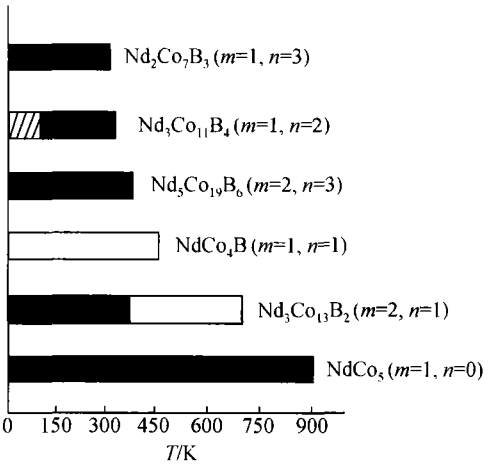

Fig. 6 Magnetic diagram of compounds $Nd_{m+n}Co_{5m+3n}B_{2n}$. □, Easy-axis anisotropy, ▨, easy-cone anisotropy, ■, basal-plane anisotropy.

Table 5 The lattice parameters, Curie temperature T_C, saturation magnetization M_s and spin reorientation temperature T_{SR} of $Nd_3Co_{13-x}Ni_xB_2$ as Ni concentration

x	a/Å	c/Å	v/Å^3	T_C/K	T_{SR}/K	M_s/(5K) (μ_B/fu)	μ_{Co} (μ_B)	EMD
0	5.0722	10.7840	240.27	710	370	20.8	0.91	Plane→axis
1	5.0690	10.8060	240.46	660	340	19.7	0.89	Plane→axis
2	5.0660	10.8270	240.64	600	300	18.3	0.85	Plane→axis
3	5.0630	10.8500	240.87	520	270	17.4	0.84	Plane→axis
4	5.0600	10.8690	241.00	480	240	16.5	0.83	Plane→axis
5	5.0565	10.8813	240.94	420	210	15.6	0.82	Plane→axis

Figure 7 gives the M-T curve determined by the vibrating sample magnetometer and shows that below the Curie temperature all the samples have the spin reorientations. The Curie temperatures T_C and the spin reorientation temperatures T_{SR} of $Nd_3Co_{13-x}Ni_xB_2$ compounds are shown in Table 5. Both T_C and T_{SR} decrease linearly with the increase of Ni contents.

Figure 8 shows that at room temperature, the XRD patterns of $Nd_3Co_{13-x}Ni_xB_2$ compounds aligned in the magnetic field. At room temperature, EMD for samples with $x = 0$ and $x = 1$ are in basal-plane. The EMD for the sample with $x = 2$ is parallel to (103) and (113) and easy-axial for samples $x \geqslant 3$. It means that they are axial anisotropic as well for samples with $x = 0$ and $x = 1$ above T_{SR}. The spin reorientation temperature corresponds to the temperature at which the EMD changes from easy basal-plane anisotropy to easy-axis anisotropy. T_{SR} of the sample with $x = 2$ is 300 K. The XRD patterns at room temperature correspond to the change of EMD from easy basal-plane anisotropy

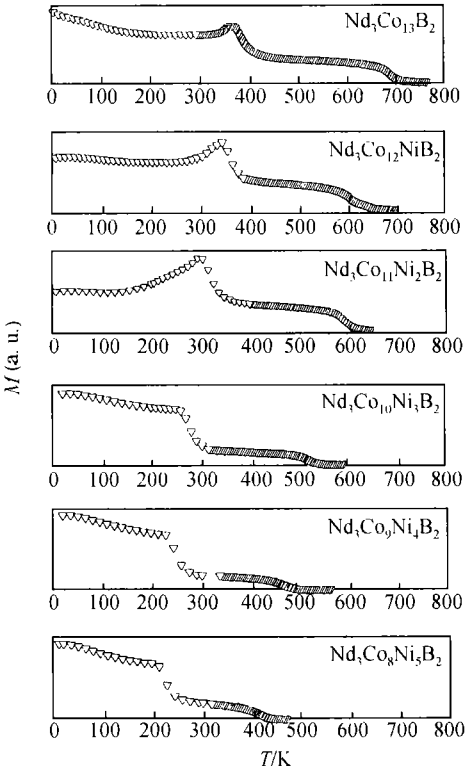

Fig. 7 Magnetization-temperature curves of $Nd_3Co_{13-x}Ni_xB_2$ ($x = 0, 1, 2, 3, 4, 5$) powders under a field of 0.05 T.

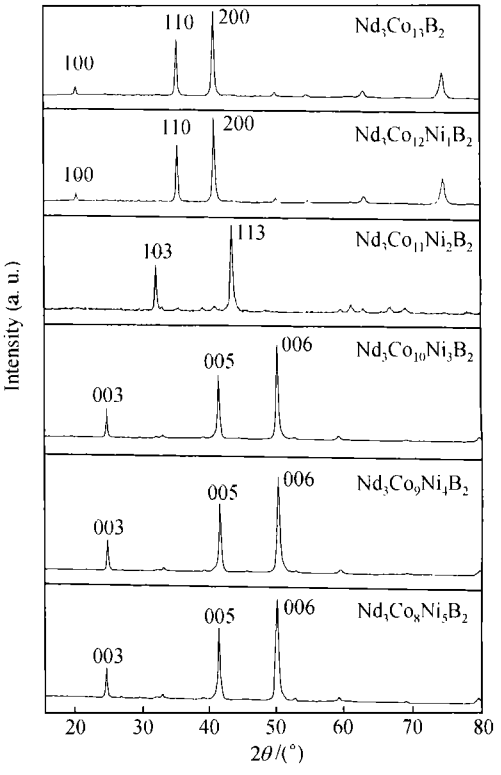

Fig. 8 XRD patterns of magnetically aligned $Nd_3Co_{13-x}Ni_xB_2$ ($x = 0, 1, 2, 3, 4, 5$) at room temperature.

to easy-axis anisotropy.

Figure 9 shows the magnetization curve $M(H)$-H of $Nd_3Co_{13-x}Ni_xB_2$ ($x = 0, 1, 2, 3, 4, 5$) powders determined by an extraction sample magnetometer. The saturated magnetization intensity M_s can be attained by extrapolating the M-$1/H$ curves to $1/H = 0$. The results are shown in Table 5. M_s decreases monotonically with the increase of amount of Ni which partially substitutes Co. At low Ni contents ($x \leqslant 2$), M_s decreases more quickly with the increase of Ni content at the beginning, then it decreases linearly. The introduction of Ni leads to not only the magnetic dilution but also reduction in the interaction of Co-Co pairs. Due to these two points, the Curie temperature T_C and the saturated magnetization intensity M_s decrease with the increase of Ni content.

4 Discussion

$R_{m+n}Co_{5m+3n}B_{2n}$ compounds with $m = 2$ have been obtained by long-time annealing at low temperature or by annealing noncrystalline samples at appropriate temperature. When anisotropic field H_A is kept at a high level, for $R_{m+n}Co_{5m+3n}B_{2n}$ compounds with the same n, T_C and M_s increase with m. With appropriate element substitutions, EMDs of $R_{m+n}Co_{5m+3n}B_{2n}$ may change from basal-

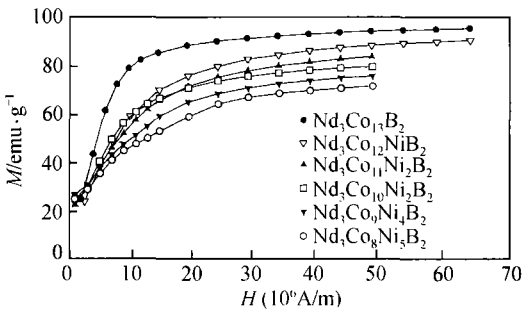

Fig. 9 Magnetization curves of random $Nd_3Co_{13-x}Ni_xB_2$ ($x = 0, 1, 2, 3, 4, 5$) powders at 5 K.

plane anisotropic to easy-axis anisotropic at room temperature. The compounds $(R_1, R_2)_{m+n}(Co, M)_{5m+3n}B_{2n}$ and their derivatives are the probable candidates for permanent magnetic materials.

The possible ways of synthesizing $R_{m+n}Co_{5m+3n}B_{2n}$ to improve T_C and M_s are as follows:

(i) The precusors RCo_5, $R_3Co_{13}B_2$ and RCo_3B_2 are prepared first, then mixed in demanded ratios and put in the ball mill to be ground into fine powder or nonocrystalline powder. The next stage is to press the mixture into disk-like samples and then anneal it at proper temperature or continue the grinding process for alloying. New compounds in $R_{m+n}Co_{5m+3n}B_{2n}$ family with $m \geqslant 2$ might be synthesized by structure combination through common plane of 3g equivalent points of P6/mmm space group.

(ii) Noncrystalline samples may be obtained by melting the materials with composition of $R_{m+n}Co_{5m+3n}B_{2n}$ ($m > 2$) at high temperature and quenching. New compounds are expected when these noncrystalline samples are annealed at appropriate temperature.

(iii) Another route to enhance the saturated magnetization is the substitution of Fe for Co because the atomic magnetic moment of Fe is much higher than that of Co. Although RFe_5 with the structure of $CaCu_5$ does not exist, Fe and rare earth can form R_2Fe_{17}, the derivative of $CaCu_5$. It possesses the same crystallographic planes as that of $CaCu_5$ in which 3g equivalent positions are located. From the point of view of structure, the combination of $mR_2(Fe,Co)_{17} + nRCo_3B_2$ seems to be worth trying.

In addition, the mutual substitution of rare earth elements plays an important role in improving the magnetic properties, especially the preferred direction of magnetization.

Acknowledgements The authors would like to thank Mr. Wei Zhifeng for editing the manuscript.

References

1 Sagawa, M. et al. New material for permanent magnets on a base of Nd and Fe (invited). J. Appl. Phys., 1984, 55: 2083.
2 Croat, J. J. et al. Pr-Fe and Nd-Fe base materials: a new class of high-performance permanent magnets (invited). J. Appl. Phys., 1984, 55: 2078.
3 Ido, H. et al. Magnetic study of $Sm_{n+1}Co_{5+3n}B_{2n}$ ($n = 0, 1, 2, 3$) in a pulsed high field. Physica B, 1992, 177: 265.
4 Ido, H. et al. New magnetic material based on $SmCo_4B$. J. Appl. Phys, 1994, 76: 6165.
5 Kuzma, Yu. B. et al. Phase diagram of R-Co-B systems. Izv. Akad, Nauk. SSSR, Neorg. Mater., 1974, 10: 265 and 2223; 1977, 13: 923; 1980, 16: 832; 1983, 19: 487 and 1757; 1988, 24: 1485.
6 Chen, Y. et al. The ternary system Nd-Co-B. J. Alloys and Compounds, 1999, 288: 170.
7 Chen, Y. et al. The ternary system Pr-Co-B. J. Alloys and Compounds, 1999, 289: 96.
8 Chen, Y. et al. Phase relation in the system Gd-Co-B. J. Alloys and Compounds, 2000, 296: L1.
9 Chen, Y. et al. Phase relation in the system Sm-Co-B. J. Alloys and Compounds, 2000, 305: 216.
10 Chen, Y. et al. Crystallographic and magnetic properties of intermetallic compound $Nd_3Co_{13}B_2$. Appl. Phys. Lett., 1999, 74: 856.
11 Chen, Y. et al. Syntheses and magnetic properties of $R_{m+n}Co_{5m+3n}B_{2n}$ compounds. J. Phys: Condens. Matter., 1999, 11: 8251.

12 Chen, Y. et al. Syntheses and magnetic properties $Pr_5Co_{19}B_6$. Phys. Rev. B, 2000, 6: 3502.
13 Chen, Y. et al. Phase relation, crystal structure and magnetic properties of Nd-Co-B borides. Chem. Materials, 2000, 12: 1240.
14 Legvold, S. et al. Rare earth metals and alloys. in Handbook of Ferromagnetic Materials, 1980, 1: 1813.
15 Ito, T. et al. Magnetocrystalline anisotropy and spin reorientation in $Gd_{1-x}Dy_xCo_4B$. J. Appl. Phys., 1996, 79: 5507.
16 Ido, H. et al. Magnetic susceptibility of RCo_3B_2 (R = Y, Sm, Gd, Dy). J. Appl. Phys, 1994, 75: 7140.
17 Aoki, M. et al. Electronic structure and magnetism of C15 type Lavers phase compounds $Y(Co,Al)_2$ and $Y(Co,Si)_2$. Physica B, 1992, 177: 259.
18 Chen, Y. et al. Structure, exchange interaction and magnetic phase transition of $Nd_3Co_{13-x}Ni_xB_2$ intermetallic compounds. IEEE Trans. Magn., 2000, 36(4): 2037.